

UNIVERSIDADE ESTADUAL DE CAMPINAS
SISTEMA DE BIBLIOTECAS DA UNICAMP
REPOSITÓRIO DA PRODUÇÃO CIENTÍFICA E INTELECTUAL DA UNICAMP

Versão do arquivo anexado / Version of attached file:

Versão do Editor / Published Version

Mais informações no site da editora / Further information on publisher's website:

<https://www.tandfonline.com/doi/full/10.1080/01932691.2019.1678482>

DOI: 10.1080/01932691.2019.1678482

Direitos autorais / Publisher's copyright statement:

©2019 by Taylor & Francis. All rights reserved.

DIRETORIA DE TRATAMENTO DA INFORMAÇÃO

Cidade Universitária Zeferino Vaz Barão Geraldo

CEP 13083-970 – Campinas SP

Fone: (19) 3521-6493

<http://www.repositorio.unicamp.br>



Dense lamellar scaffold, biomimetically inspired, for reverse cardiac remodeling: Effect of proanthocyanidins and glutaraldehyde

Thais Alves, Juliana Ferreira Souza, Venancio Alves Amaral, Alessandra Candida Rios, Tais Costa, Kessi Crescencio, Fernando Batain, Denise Grotto, Renata Lima, Lindemberg Silveira Filho, Jose Oliveira Junior, Patricia Severino, Norberto Aranha & Marco Chaud

To cite this article: Thais Alves, Juliana Ferreira Souza, Venancio Alves Amaral, Alessandra Candida Rios, Tais Costa, Kessi Crescencio, Fernando Batain, Denise Grotto, Renata Lima, Lindemberg Silveira Filho, Jose Oliveira Junior, Patricia Severino, Norberto Aranha & Marco Chaud (2019): Dense lamellar scaffold, biomimetically inspired, for reverse cardiac remodeling: Effect of proanthocyanidins and glutaraldehyde, Journal of Dispersion Science and Technology, DOI: [10.1080/01932691.2019.1678482](https://doi.org/10.1080/01932691.2019.1678482)

To link to this article: <https://doi.org/10.1080/01932691.2019.1678482>



Published online: 16 Oct 2019.



Submit your article to this journal [↗](#)



Article views: 48







View related articles [↗](#)



View Crossmark data [↗](#)

Dense lamellar scaffold, biomimetically inspired, for reverse cardiac remodeling: Effect of proanthocyanidins and glutaraldehyde

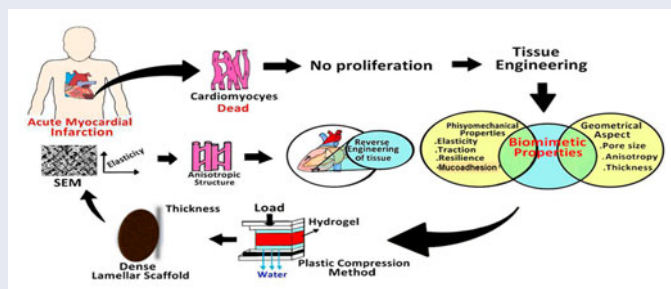
Thais Alves^a , Juliana Ferreira Souza^a, Venancio Alves Amaral^a , Alessandra Candida Rios^a, Tais Costa^b, Kessi Crescencio^a, Fernando Batain^a, Denise Grotto^c , Renata Lima^b, Lindemberg Silveira Filho^d, Jose Oliveira Junior^e, Patricia Severino^f , Norberto Aranha^g, and Marco Chaud^a

^aLaboratory of Biomaterials and Nanotechnology, University of Sorocaba, Sorocaba, São Paulo, Brazil; ^bLaboratory of Bioactivity Assessment and Toxicology of Nanomaterials, University of Sorocaba, Sorocaba, São Paulo, Brazil; ^cLaboratory of Toxicological Research, University of Sorocaba, Sorocaba, São Paulo, Brazil; ^dMedical Science College, University of Campinas, Campinas, São Paulo, Brazil; ^eLaboratory of Physical Nuclear, University of Sorocaba, Sorocaba, São Paulo, Brazil; ^fLaboratory of Nanotechnology and Nanomedicine, University of Tiradentes, Tiradentes, Brazil; ^gTechnological and Environmental Processes, University of Sorocaba, Sorocaba, São Paulo, Brazil

ABSTRACT

Regenerative medicine is an emerging field that aims in healing damaged tissue. The choice of the crosslinking agent is one of the most critical requirements for the development of three-dimensional scaffold devices. This study aimed to investigate the effects of proanthocyanidins (PA) and glutaraldehyde (GA) associated with plastic compression method on the properties of the dense lamellar. The biomechanical and physical-chemical properties of the scaffolds were evaluated. The antioxidant activity was investigated by 2,2-diphenyl-1-picrylhydrazyl method; viability and proliferation cellular were evaluated by 3-(4,5-dimethylthiazolyl-2)-2,5-diphenyltetrazolium bromide and imaging cytometer (H9c2 cells). The effect of the crosslinking agents modified the biomechanical properties but did not modify the mucoadhesion properties. Proanthocyanidin-scaffold has the ability to bind water's molecule and to reduce the space between polymeric chains. Proanthocyanidin-scaffold and GA scaffold showed, respectively, 44 and 17% of antioxidant activity. Both crosslinking agents did not influence the viability and proliferation of H9c2 cells. Considering the anisotropic structure, and the biomechanical properties, cellular compatibility, and protective action against reactive oxygen species, this study may provide a way to improve the inverse modulation of heart tissue, after infarct acute of the myocardium.

GRAPHICAL ABSTRACT



HIGHLIGHTS

- Tissue engineering has emerged as a promising alternative for cardiac regeneration.
- Dense lamellar scaffolds were obtained by plastic compression method.
- Crosslinking agent was important to modulate the physicochemical properties.
- Biomimetic properties as anisotropy and elasticity were obtained.
- The study may provide a way to improve the inverse remodulation of heart tissue.

Introduction

Cardiovascular disease is one of the most severe health problems in the world, and it yields a high level of mortalities every year. Normally, heart failure is the final common

stage of most types of cardiovascular disease, preceded by myocardial infarction, hypertension, arrhythmia, and a variety of cardiomyopathies. Heart muscle cells lose their capacity to divide early after birth. The loss of a relevant

fraction of myocytes (e.g., during myocardial infarction) leads to a permanent reduction in contractile function and eventually heart failure.^[1,2]

Regenerative medicine is an emerging field that aims in improving or repairing the performance of damaged tissue or organ. Numerous strategies, including the use of materials and cells, as well as various combinations thereof, to take the place of missing tissue, effectively replacing it both structurally and functionally, or to contribute to tissue healing.^[3,4]

Scaffolds are three-dimensional (3D) and porous structures that can be produced using biopolymers able to mimic the extracellular matrix (ECM). The scaffolds should be able to mechanically support the native tissue during the necessary time of regeneration repair, and it also plays an important role in providing essential signals to cell activities. The choice of biomaterials and the selection of the experimental conditions for the design of these scaffolds are important parameters to assuring the appropriate setting for cell's growing and proliferation into the 3D matrices.^[5–7] Based on this concept, cardiac tissue engineering has been introduced as a promising technique to benefit patients with cardiovascular disease.^[1]

The stiffness of myocardial is between 10–20 kPa earlier of diastole, and 200–500 kPa at the ending of diastole. Although the materials should be designed to be proportional to the fractional volume of the scaffolds, the use of stiffer materials can contribute to attenuate the stress in the cardiac wall.^[8]

Proteins and polysaccharides are considered promising natural molecules for the design of 3D scaffolds with biomimetic characteristics of original tissue. Type I collagen makes up about 80% of the collagen matrix in cardiac tissue, making this biopolymer an attractive for the manufacture of scaffolds for cardiac tissue. Collagen in combination with other biomaterials such as chitosan showed an increase in the elastic modulus, which makes it more suitable for the stabilization of the ventricular wall. Chitosan (Qt) is a natural polymer composed of glucosamine and *N*-acetylglucosamine. A chitosan hydrogel has been designed, which improved the survival of embryonic stem cells and the differentiation of cardiomyocytes in a rat infarction model.^[9–11]

The silk fibroin (SF) is a natural polymer with biomedical applications due to its characteristics of oxygen and water permeability, cell adhesion and growth, low thrombogenicity and inflammatory response, and high tensile strength with flexibility.^[12] Hyaluronic acid (HA) is a natural polysaccharide which, together with collagen, is one of the most abundant components of ECM. In addition, HA-containing devices offer advantageous properties such as bioresorbable, inhibition of scar formation, and the promotion of angiogenesis.^[13]

The major problem associated with collagen gel for myocardial use is its low density; thus it occupies a large volume.^[14] The plastic compression, where the collagen gels are subjected to uniaxial compression using a strain rate, forcing free water out of the matrix in the transverse plane and densifying the network of collagen fibrils. The result is

a dense and thin gel with collagen fibrils aligned (anisotropic form). This process associated with freeze-drying can produce a dense lamellar scaffold with an increase of the mechanical properties and biomimetic function to original tissue.^[15]

Collagen scaffolds produced by plastic compression technique associated with photochemical crosslinking that has shown an increase mechanical stability reduce the swelling rate and increase the time of the disintegration.^[16,17]

The crosslinking technology is one of the most important areas of research focusing on the development of new tissue engineered that use the proteins and polysaccharides as polymers.^[18] A crosslinking agent can be physical or chemical origin, and both are able to connect the functional groups of the polymer chain to another one through covalent bonding or supramolecular interactions such as ionic bonding or hydrogen bonding. This crosslink can affect some physicochemical properties including mechanical properties such as tensile strength, stiffness, and strain, cell-matrix interactions, performance at higher temperatures, resistance to enzymatic and chemical disintegration, gas permeation reduction, and shape memory retention of the products.^[18,19]

An ideal crosslinking agent should not be cytotoxicity for the myocardium. The crosslinking agent could improve the mechanical performance of the materials and inhibit calcification of the infarcted area. The crosslinking agents for scaffolds may be classified as chemical crosslinking agents (carbodiimide, epoxy compounds, and glutaraldehyde) and natural crosslinking agents (genipin, nordihydroguaiaretic acid, tannic acid, and procyanidins). Many aspects of the natural substances as crosslinking agents have better quality than the chemical crosslinking agents, especially in terms of cytotoxicity and anticalcification ability.^[20,21] The plastic compression associated with a chemical crosslinking agent has not related by literature.

Proanthocyanidins (PA) are polyphenolic compounds known as condensed tannins. Proanthocyanidin is a natural product with a polyphenolic structure that has the potential to give rise to stable hydrogen-bonded structures and generate nonbiodegradable collagen matrices. Mechanisms for interaction between PA and proteins include covalent interactions, ionic interactions, hydrogen-bonding interactions, or hydrophobic interactions.^[16] The stability of these crosslinks compared with other polyphenols suggests a structure specificity, which encourages hydrogen binding and creates hydrophobic pockets. Proline is an amino acid with carbonyl oxygen adjacent to secondary amine nitrogen and it is hydrogen acceptor. The proline (proteinogenic amino acid) contributes to the formation of the collagen, and by means of the hydrogen bonds, it presents high affinity for PA [(Formatting Citation)].

In addition, the PA possesses antibacterial, antiviral, anti-inflammatory, antiallergic, and vasodilatory actions. Furthermore, PA has capacity to inhibit lipid peroxidation, platelet aggregation, and the permeability and fragility capillary. Proanthocyanidins have been shown to modulate the activity of regulatory of the enzyme lipoxygenase, protein

Table 1. PA-scaffold and GA-scaffold formulations.

	PA-scaffold	GA-scaffold
Collagen	1.0 g	1.0 g
Chitosan hydrogel (3%)	1.0 g	1.0 g
Poloxamer 407	0.06 g	0.06 g
Proanthocyanidin	0.08 g	–
Glutaraldehyde (25% H ₂ O)	–	0.08 g
Hyaluronic acid (1 %)	0.06 g	0.06 g
Fibroin solution	4.0 mL	4.0 mL
Polyethylene glycol 400 (3%)	2.0 mL	2.0 mL
DMEM	4.0 mL	4.0 mL
H ₂ O ultrapure	8.0 mL	8.0 mL

kinase C, cyclooxygenase, angiotensin-converting enzyme, hyaluronidase, and cytochrome P450 activities.^[22,23]

Glutaraldehyde (GA) has been extensively used as a chemical crosslinking agent to crosslink various types of biopolymeric for tissue scaffolds, hydrogels, and composites.^[24–28] Glutaraldehyde reacts with the amine or hydroxyl functional groups of proteins and polymers, respectively, through a Schiff-base reaction and connects the biopolymeric chains via intra- or intermolecular interactions. Therefore, all the available free amine groups which are present in the chemical structure of protein molecules such as gelatin, react with GA, forming a more strongly crosslinked network.^[18,29]

Although PA crosslinked collagen scaffold has been studied in a previous study,^[18,19,30,31] to date no other studies have been conducted using plastic compression in association to improve the mechanical properties as well as cellular behaviors on GA as a crosslinking agent for collagen 3D porous scaffolds. This study aimed to investigate the effects of PA and GA associated with plastic compression on the properties of the dense lamellar scaffold. Moreover, the dense lamellar scaffolds should have proper characteristics about biomechanical properties, swelling, anisotropic degree, disintegration, antioxidant activity, and cytotoxicity. The polymers used to modulate the properties of dense lamellar scaffolds were collagen, fibroin, chitosan, HA, Poloxamer 407, and polyethylene glycol 400.

Materials and methods

Materials

Collagen powder type I was supplied by NovaProm Food Ingredients Ltda. (Brazil). Deacetylate (75–85%) chitosan of average molar mass, glutaraldehyde, poloxamer 407, and DMEM were purchased from Sigma-Aldrich Co. (USA). Proanthocyanidin was purchased from GAMA Ltda. (Brazil). Hyaluronic acid was purchased from Via Farma Ltda. (Brazil). Polyethylene glycol 400 was purchased from Dinamica Ltda. (Brazil). The other reagents were of pharmaceutical grade. All samples were used without any chemical treatment.

Preparation of fibroin solution

Bombyx mori SF was prepared after removing of the sericin by autoclaving (120 °C, 15 minute and 1 atm.) of silk

cocoons in an aqueous solution of Na₂CO₃ 0.5 wt%.^[32] The SF was soaked methodically in water to extract the residual sericin. The degummed SF was dissolved in CaCl₂·2H₂O/CH₃CH₂OH/H₂O solution (mole ratio, 1:2:6) at 85 °C. The solution was filtered, transferred to a dialyzer tubing with a molecular weight cutoff 14,000, and dialyzed against distilled water for 72 hours to yield fibroin solution (SF). The fibroin concentration determined by weighing the remaining solid after drying was 2.7 wt%.

Preparation of hydrogel crosslinked with PA or GA

Formulations of the hydrogels for the manufacturing of scaffolds crosslinked with PA or GA are summarized in Table 1. The collagen dispersion was prepared with 2 mL of DMEM, 1 g of collagen type I (COL), and enough ultrapure water to obtain 10 mL of dispersion. In preparation of hydrogel formulation, the solution of fibroin (SF), Polyethylene glycol 400 (PEG), Poloxamer 407 (P407), hydrogel chitosan (CH) previously prepared with CH of average molecular weight,^[33] and crosslinking agent (PA or GA) were added to the collagen dispersion following this order. The mixture of the compound was done by mechanical stirring until obtaining a uniform hydrogel.

Thereafter, the pH of the formulation was adjusted to 10 using NaOH (2M) and added HA to the polymer dispersion. To complete the polymerization reaction, the colloidal dispersions were left at 10 °C for 24 hours into a cylindrical mold with capacity for 4.0 cm³, to become a thick solid-looking gel.

Preparation of dense lamellar scaffolds

Dense lamellar scaffolds were produced by plastic compression (using a hydrostatic press), as described by our group in a previously published article.^[33] Briefly, the thick solid-looking gel was placed on a porous support, assembled, from bottom to top, with absorbent paper layers, one steel mesh, and two nylon meshes. Subsequently, a static compressive load of 4 kN was applied for 10 minutes to the thick solid-looking gel to remove water and produce a dense biomaterial slightly hydrated and improved biological and mechanical properties. Finally, the matrices were freeze-dried, resulting in a low-density crosslinked scaffold.

Physiomechanical and mucoadhesive properties

Texture profile analysis (TPA) was used to measure the physiomechanical properties (elasticity, flexibility, drilling, and resistance to traction) of scaffolds. The tests were performed using a Stable Micro Systems Texture Analyzer (Model TA-XT Plus) in texture profile analysis mode with a load cell of 5 kg. This process was previously described by Alves et al.^[33] Briefly, the samples scaffolds, with approximately 40 mm of diameter, were hydrated for 1 hour. The excess of the water of scaffolds was removed and fixed in suitable apparatus to each analyzation. The speeds of the tests were previously defined for a rate of 2 and 0.5 mm.

s^{-1} , respectively, for drilling and resistance to traction, and elasticity and flexibility. Elastic (Young's) modulus was obtained by compression and tension until densification of the sample. The Elastic modulus was calculated with a strain ranged between 0 and 5%.

The mucoadhesive properties of scaffolds were evaluated using a Stable Micro Systems Texture Analyzer (Model TA-XT Plus) using mucin disks. The mucin disks were prepared for compression (Lemaq, Mini Express LM-D8, Brazil) with flat punches, and cylindrical matrix with diameter of 8 mm, and a compaction load of 8 ton. This process was previously described, briefly, the mucin disks with a thickness of 0.2 mm were previously hydrated and attached to the lower end of the analytical probe.^[33] The scaffold samples with 40 mm of diameter were fixed in a suitable apparatus. Mucin disk attached in the probe was compressed on the surface of the scaffold with a force of 0.098 N, directed in the apical → basal way. Contact time between mucin disk and the sample was of 100 seconds, (this time was previously established in a prequalification study and has been considered great to perform an intimate contact of the mucin disk with the sample). The test was performed with a constant speed of 10 mm.s^{-1} . The force required to detach the mucin disk from the surface of the scaffold was determined from the time (s) × force (N) ratio.

Swelling efficiency

The scaffolds were cut in the square shape ($15 \times 15 \text{ mm}$), weighed, and then immersed in 3 mL of PBS (phosphate buffer saline, pH 7.4) at 37°C for up to 14 days. As described at different time points, the samples were removed, and different measurements to evaluate the capacity to retain PBS fluid were made. The first measurement was aimed at assessing the ability of the scaffold structure as a whole (i.e., the material itself together with the pore system) to absorb the PBS. For this, at each time point, the samples were removed from fluid, shaken gently, and then weighed without dripping (Wws). The second measurement was carried out after pressing and “drying” the same soaked samples between sheets of filter paper to remove the water retained in its porous structure (Wwm).^[3] In this way, the swelling ability of scaffold material itself was determined. The scaffolds were then dried at 37°C until constant weight was reached (Wd).^[33] The percentage of fluid uptake, in both cases, was calculated as shown (Equation 1)^[3]:

$$\text{Fluid uptake of scaffolds (\%)} = \left(\frac{W_w - W_d}{W_d} \right) \times 100 \quad (1)$$

where W_w represents Wws or Wwm, and W_d is dry scaffold. Each sample was measured in triplicate.

In vitro degradation study

Proanthocyanidin-scaffold and GA-scaffold were hydrated in PBS at 37°C to evaluate their degree of degradation. Scaffolds were cut to square shape ($15 \times 15 \text{ mm}$), weighed prior to the degradation study (W_d'), and then immersed in

3 mL of PBS at 37°C for up to 14 days. At different time points, they were removed, washed in a large volume of deionized water to remove buffer salts, and dried at 37°C until constant mass was reached. Finally, the samples were weighed (W_a) and the percentage weight loss was calculated as follows (Equation 2):

$$\text{Weight loss (\%)} = 100 \times \left(\frac{W_d' - W_a}{W_d'} \right) \quad (2)$$

The pH value of the PBS was measured at each time point using a pH-meter (Tecnal, TE-5, Piracicaba, Brazil). Each sample was measured in triplicate.

Porosity, interconnectivity, and pore size

The morphometric characteristics of the porosity, interconnectivity, and pore size of scaffolds were evaluated by computerized microtomography (μCT). The scaffolds pictures were captured by XRay microtomography (Brucker-micro CT – Sky-Scan 1174, Belgium) with resolution scanner of the 28 mM pixel and integration time at 1.7 seconds. The source of the X-rays was 35 keV and 800 μA of current. The projections were acquired in a range of 180° with an angular step of 1° of rotation. Three-dimensional virtual models' representative of various regions of scaffolds were created, and CT Analyzer (v. 1.13.5) mathematically treated the data.^[34]

Specific permeability measurement

Specific permeability was measured using a device previously described by Varley et al. and Gilmore et al.^[35,36] to maintain a constant, respectively, the pressure gradient across of collagen scaffold and bone scaffold, which was defined by the hydrostatic water ($\Delta P = r.H.g$), where basal face of scaffold was exposed to the atmosphere and the apical face was in contact with water column. The pressure was held constant across the scaffold (thickness scaffold = L) and the volumetric flow rate (Q) of distilled water across the scaffold was measured (from the mass of water passing through the scaffold in a given time). This mass was measured, using a balance with a precision of 1 mg, and converted to volumetric flow using the fluid density ($\rho = 0.998 \text{ mg m}^{-3}$). From Q , the sectional area (A) and the pressure gradient, $\Delta P/L$, the specific permeability, k , was calculated using Darcy's Law (Equation 3)^[36]:

$$k = \frac{Q \cdot L \cdot \mu}{A \cdot H} \quad (3)$$

in which h , the dynamic viscosity, has units of Pa s and k has units of m^2 . The viscosity of the water was taken as $8.9 \times 10^{-4} \text{ Pa.s}$. A total of three samples with 1.5 cm diameter were used. The water column (H) was 56 cm. Furthermore, a press fit mount was used to prevent scaffold deformation. The mount aperture was slightly larger than the scaffold diameter in the dry state. When hydrated, the scaffold expanded to fill the entire aperture.

Scanning electron microscopy

Scanning electron microscopy (SEM) photographs scaffolds were obtained using a scanning electron microscope (LEO Electron Microscopy/Oxford, Leo 440i, England) with a 10 kV accelerating voltage. Scaffold samples were previously frozen with liquid nitrogen, cut out (dimension, 30×30 mm) and mounted on pins stubs specimen using carbon double-sided adhesive tape. The samples were sputtered coated with gold for 4 minutes at 15 mA, using SC7640 Sputter-Coater.

Differential scanning calorimetry

Differential scanning calorimetry (DSC) was performed on a Shimadzu, TA-60, Japan, previously calibrated using indium as the reference material. A sample of 2 mg was packed in a hermetically crimped aluminum pan and heated under dry nitrogen purged at 30 mL min^{-1} . The samples were heated from 25 to 350°C at a rate of $10^\circ\text{C min}^{-1}$.^[33,37]

Fourier transform infrared spectroscopy

Fourier transform infrared spectroscopy (FTIR) analysis (Shimadzu, IRAffinity-1, Japan) was used to collect FTIR spectra by LabSolutions Software v.2.10. The stretches of the chemical bonds of the main functional groups of each molecule making up the sample were determined by an attenuated total reflectance (ATR) over the range between 4000 and 600 cm^{-1} at 4 cm^{-1} resolutions, averaging 128 scans. The scaffold samples were carefully manipulated and put on the ATR-8200HA support before each analyzation.^[33]

In vitro antioxidant activity

The antioxidant activity, in vitro, of the PA-scaffolds and GA-scaffolds was determined using an ethanolic solution of 2,2-diphenyl-1-picrylhydrazyl (DPPH) 0.1 mM , as a free radical, and DPPH as radical sequestering. The absorbance was determined at a wavelength of 515 nm in a spectrophotometer (Lambda 35, PerkinElmer, USA) at 0, 15, 30, 45, and 60 min. The tubes containing the samples were kept under the light. The ability of the radical sequestering sample (DPPH), expressed as *per cent* inhibition was calculated according to Equation 4 and plotted.^[38]

$$\text{Inibição (\%)} = \frac{\text{Abs1} - \text{Abs2}}{\text{Abs1}} \times 100 \quad (4)$$

Cell viability

Initially, the extract of scaffold was made using a 1 cm^2 scaffold fragment in 2.5 mL culture medium for 24 hours. After this time, the total cell adhesion treatments were performed using the extracts at 100, 50, and 25% dilutions, and were maintained for 24 hours. Approximately, 5×10^5 cells/well (H9c2 cells – cardiac myoblasts) were plated in 96-well plates. The culture medium was removed and $100 \mu\text{L}$ of

MTT solution (3-(4,5-dimethylthiazolyl-2)-2,5-diphenyltetrazolium bromide) at 5 mg mL^{-1} was added to each well and maintained in 37°C for 3 hours. After this, the MTT solution was withdrawn and $100 \mu\text{L}$ of DMSO per well was added for cell attachment. The reading was performed using ELISA microplate reader at 570 nm . The concentration of material in this method is equivalent to exposing 1.6 m of material to a 70-kg individual.^[33,39]

Image cytometer

Approximately, 1×10^5 cells/well (H9c2 cells – cardiac myoblasts) were plated in a 24-well plate, at time 0 hours, and was incubated at 37°C – 5% CO_2 using Minimum Essential Alpha medium with ribonucleotides, deoxyribonucleosides, L-glutamine (2 mM) and sodium pyruvate (1 mM) to a final concentration of 10%, without ascorbic acid added of the fetal bovine serum. After 24 hours and total adhesion of the cells, they were placed in contact with the material for 48 and 72 hours.^[28,33] The samples were removed from the cultures and the cells were washed with PBS, trypsinized, and counted using the Image Cytometry technique.^[33,39]

Results

Physiomechanical and mucoadhesive properties

Figure 1A–1C shows the results of physiomechanical properties of the scaffold obtained by plastic compression, 1 hour after hydration. The PA-scaffold showed better results ($p < .05$) for drilling, flexibility, and traction properties than GA-scaffold (Figure 1A). The mucoadhesion property was similar ($p > .05$) for both scaffolds (Figure 1A). The Young's modulus (Figure 1B) results by tension were 161.23 and 179.97 KPa for PA-scaffold and GA-scaffold, respectively. The Young's modulus (Figure 1B) results by compression were 174.01 and 188.77 KPa for PA-scaffold and GA-scaffold, respectively.

The results of relaxation stress are shown in Figure 1C. PA-scaffold showed the highest level of Fmax. The high level of firmness in PA-scaffold might owes to the brittle and rigid network strand. While GA-scaffold exhibited the lower level of Fmax and this could be attributed to the PA addition that became more flexible the network strands that were able to distribute force during compression.

Swelling efficiency

The results of scaffold PBS-absorption ability are shown in Figure 2, where swelling characteristics related to fluid retained both by the whole scaffold structure (Wwd) in Figure 2A. Figure 2B shows the scaffold without PBS excess (Wwe). Both scaffolds (PA and GA) showed a high capacity for PBS uptake. However, differences in absorption were observed between the scaffolds with the PA or GA crosslinking agent. In both studies, the GA-scaffold showed, on average, a fluid retention 1.24 times bigger than PA-scaffold for 14 days.

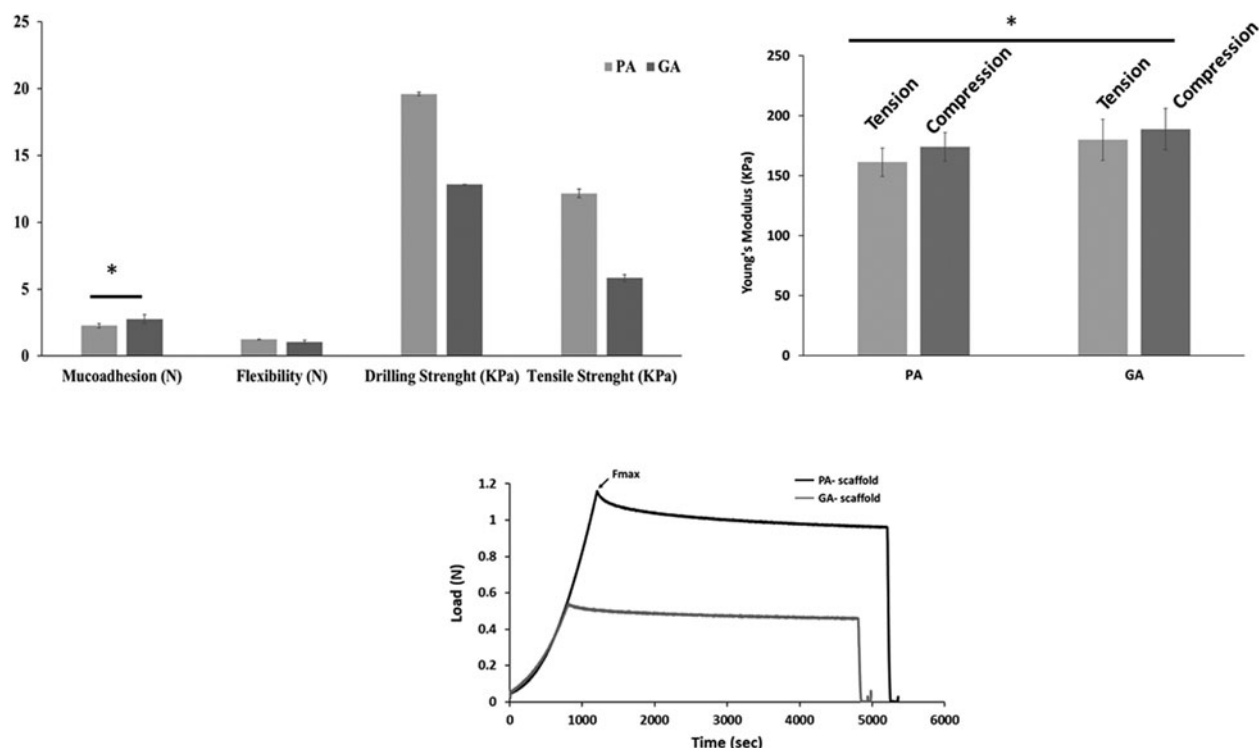


Figure 1. Physiomechanical properties of PA-scaffold and GA-scaffold. Drilling, flexibility, traction, and mucoadhesion (A). Young's Modulus test (B). Relaxation stress test (C). *Statistical equals were found between PA-scaffold and GA-scaffold ($p > .05$) ($n = 3$; bar charts represent standard deviation values).

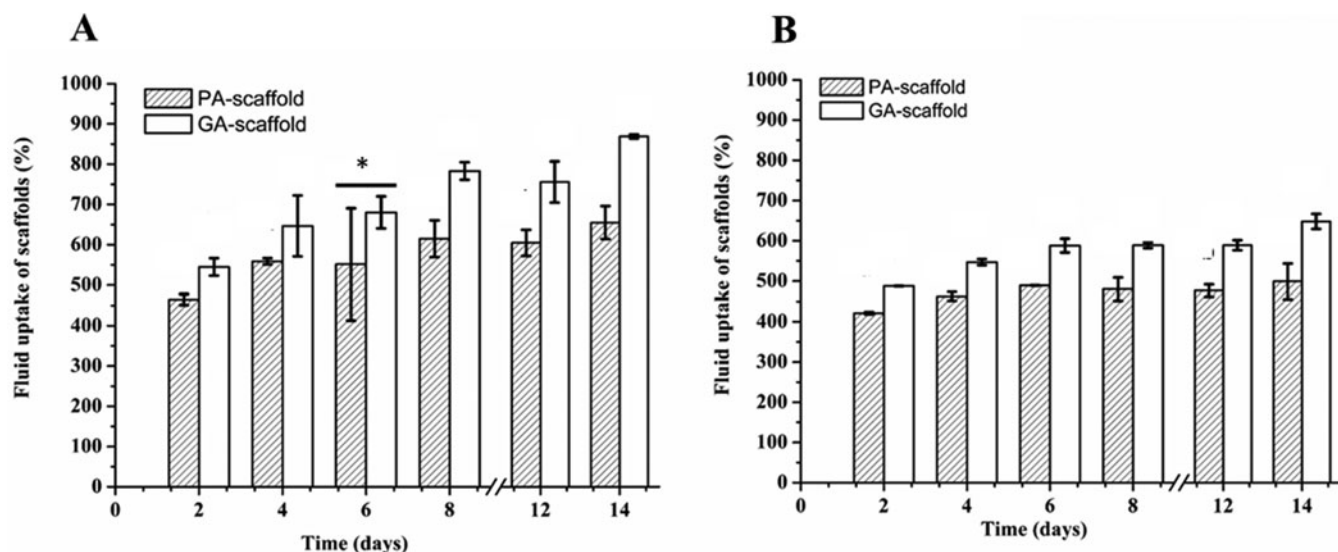


Figure 2. Fluid uptake of scaffolds (%) fluid retained both by the whole scaffold structure (A), and by the scaffold material itself (B) in PBS at 37 °C according to the crosslinking agent. *Statistical equals were found between PA-scaffold and GA-scaffold ($p > .05$) ($n = 3$; bar charts represent standard deviation values).

In vitro disintegration study

The resistance of scaffolds to disintegrate in the PBS presence, at 37 °C for 14 days was strongly dependent on the crosslinking agent, as shown in Figure 3A. For GA-scaffold (Figure 3A) the percentage of mass loss was significantly higher ($\sim 2\times$) than the PA-scaffolds. At the end of 14 days, the mass loss was approximately 20 and 9% for GA-scaffold and PA-scaffold, respectively. The hydrolytic degradation GA-scaffold and did not cause a significant change in pH value (Figure 3B), this being maintained in a range of 6.5 and 7.8 throughout 14 days of experiments.

Porosity, interconnectivity, and pore size

The morphological characteristics of PA-scaffold and GA-scaffold were obtained by μ CT and are summarized in Table 2. The pores interconnectivities of the PA-scaffold and GA-scaffold were 75.23 and 74.74%, respectively. The anisotropy is associated with lamellar characteristic on scaffolds. The use of μ CT allows to obtain the degrees of anisotropy of the scaffolds (Table 1), that can range from 0 (the structure is completely isotropic) to 1 (the structure is completely anisotropic).^[40,41] The values obtained to degrees of anisotropy of the PA-scaffold and GA-scaffold were 0.99 and 0.81,

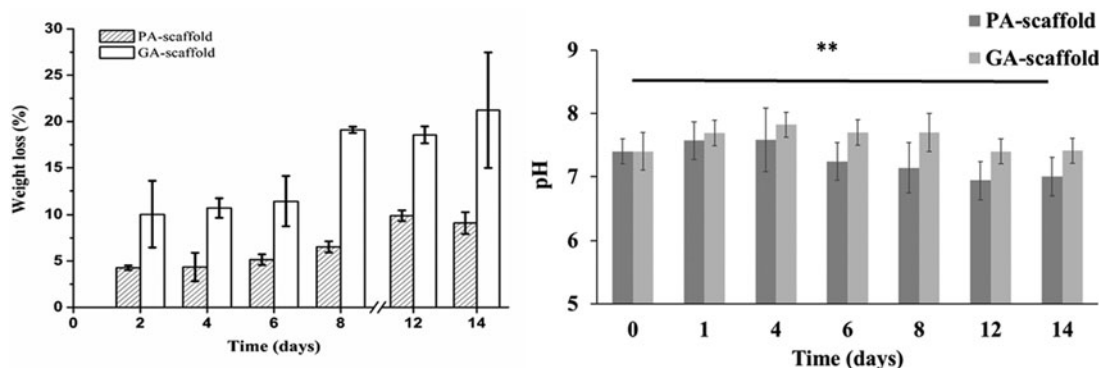


Figure 3. (A) Weight loss (%) and (B) pH of scaffolds in PBS at 37 °C according to the crosslinking agent. *Statistical equals were found between PA-scaffold and GA-scaffold ($p > .05$) ($n = 3$; bar charts represent standard deviation values).

Table 2. Morphological characteristics and anisotropy degree of scaffolds.

	PA-scaffold	GA-scaffold
Total VOI volume (mm ⁻³)	465,925	497,002
Pore interconnectivity (%)	75.23	74.74
Volume of open pores (%)	75.26	47.28
Closed porosity (%)	0.14	0.18
Anisotropy degree	0.99	0.81

respectively. Thus, the scaffolds obtained by plastic compression technique produced structures anisotropic, that is, dense lamellar scaffolds.

Permeability measurement

The permeability coefficient can be used as a quantitative tool to predict the barrier performance of porous media, and also to estimate parameters as anisotropy or isotropy of the porous. Likewise, it was possible to use the permeability of the dense lamellar scaffolds to evaluate the thickness required, and the plastic compression performance may be estimated from Equation (3). The permeability coefficient of PA-scaffold was 7×10^{-9} m², and GA-scaffold was 2×10^{-10} m². These results are coherent with the degree of anisotropy summarized in Table 2.

Scanning electron microscopy

Figure 4A and 4B compares the inner morphology of the PA-scaffold and GA-scaffold Figure 4C and 4D. A continuous structure of interconnected pores with mainly uniform distribution was obtained in the PA-scaffold, and the same did not observe for GA-scaffold. The PA-scaffold showed the uniform rectangular shape in its surface (Figure 4A and 4B), whereas the GA-scaffold showed irregular rounded shapes (Figure 4C and 4D). The pore dimensions estimated from SEM microphotographs were mostly in the range of 100–150 μ m for both scaffolds. The use of PA and fibroin in formulation associated with plastic compression technique generated the formation of the sheets in structure surface of the scaffold (Figure 4A and 4B). The same was not observed for scaffolds produced with GA as crosslinking agent, in other words, the crosslinking agents and GA produced different porous structures. The opposite result for PA and GA

structures did not significantly influence the formation of internal porous.^[19]

Differential scanning calorimetry

The DSC thermogram of excipients, PA-scaffold, and GA-scaffold is shown in Figure 5. The DSC plots give an endothermic peak associated with a helix to coil transition which indicates the extent of intermolecular crosslinking.^[42] The denaturation temperature (T_d) of PA-scaffold and GA-scaffold was near 90 °C. The miscibility can be analyzed with DSC to determine when has a single glass-transition temperature (T_g s).^[37] The T_g s at 220 °C to PA-scaffold and GA-scaffold were also observed for COL in the natural form, indicating that the blend of polymers forms a miscible blend.

Fourier transform infrared spectroscopy

Representative FTIR spectra for excipients of formulation and scaffolds are shown in Figures 6. The spectra of both scaffolds depict characteristic absorption bands in 1645 cm⁻¹ corresponding to amide I absorption arises predominantly from protein amide C=O stretching vibrations and 1545 cm⁻¹ corresponding to amide II is made up of amide N-H bending vibrations and C-N stretching vibrations. The 1240 cm⁻¹ corresponding to amide III band is complex, consisting of components from C-N stretching and N-H in-plane bending from amide linkages. The band at 1098 cm⁻¹ corresponded to the stretching vibration of the C-O bond.^[43–45]

The spectra were scaled to equal absorption at 3302 cm⁻¹ which is assigned to the -CH₂ chemical group. -CH₂ group remains unchanged during the crosslinking reaction of COL. As shown in Figure 6 it is that crosslinking of COL matrices by PA/GA has increased its intensity of transmittance at 1643 cm⁻¹ comparing to the native COL matrix. It can be concluded from increasing the intensity of transmittance at 1643 cm⁻¹ that carboxyl (-COOH) groups in COL matrix have been reduced due to the crosslinking reaction. Furthermore, it can be seen a decreased intensity of transmittance at 1082 cm⁻¹ after crosslinking of COL matrix. It can be concluded from decreasing the intensity of

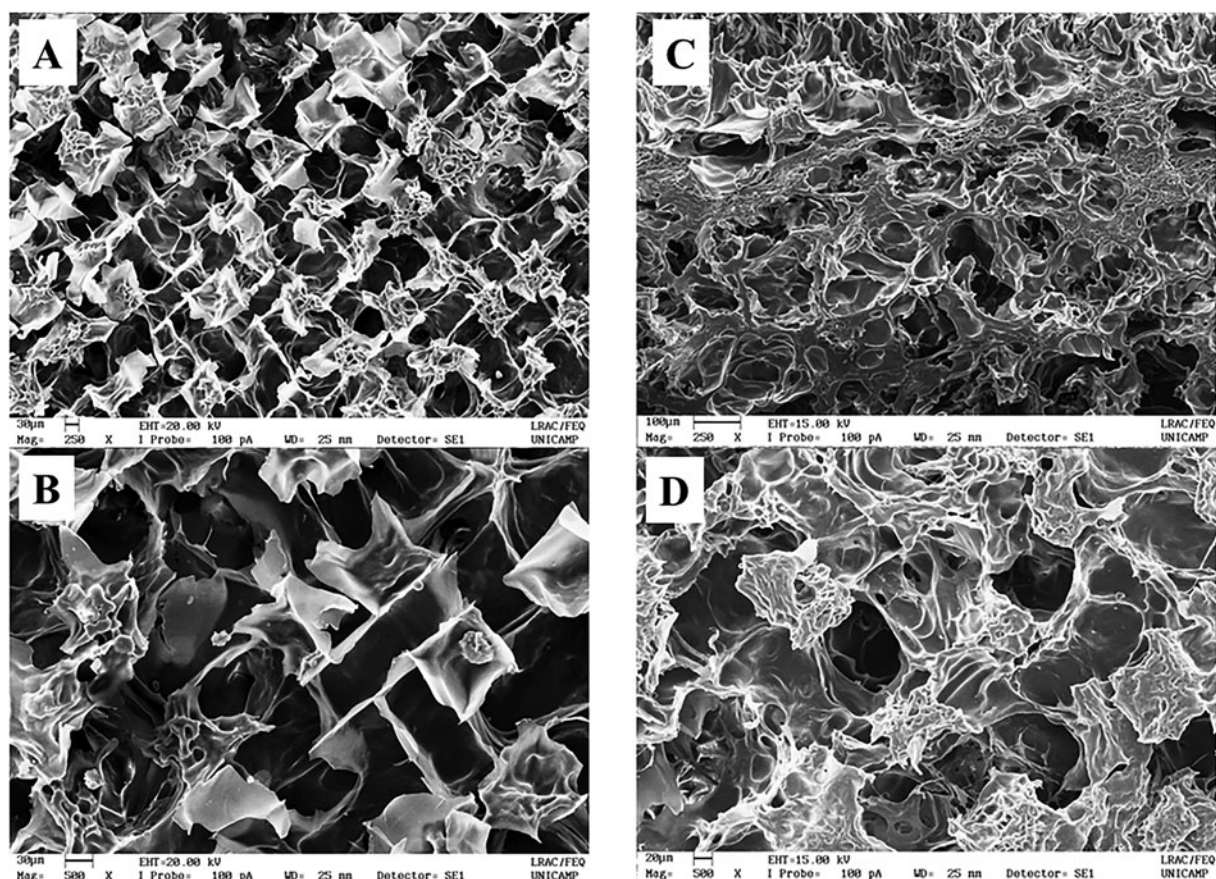


Figure 4. Scanning electron microscopy of the scaffold's samples: proanthocyanidin-scaffold (A, B) and glutaraldehyde-scaffold (C,D).

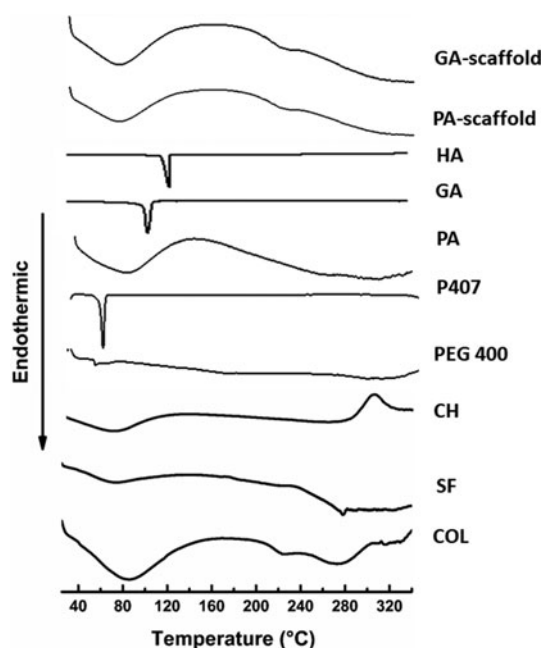


Figure 5. Differential scanning calorimetry thermogram of raw materials, PA-scaffold, and GA-scaffold.

transmittance at 1082 cm^{-1} that crosslinking of COL makes more amide bonds between COL macromolecules.

The transmittance at $\sim 1600\text{ cm}^{-1}$ is due to the amide II band, which originates from the N-H bending vibration and the C-N stretching vibration. One notes a shift in the

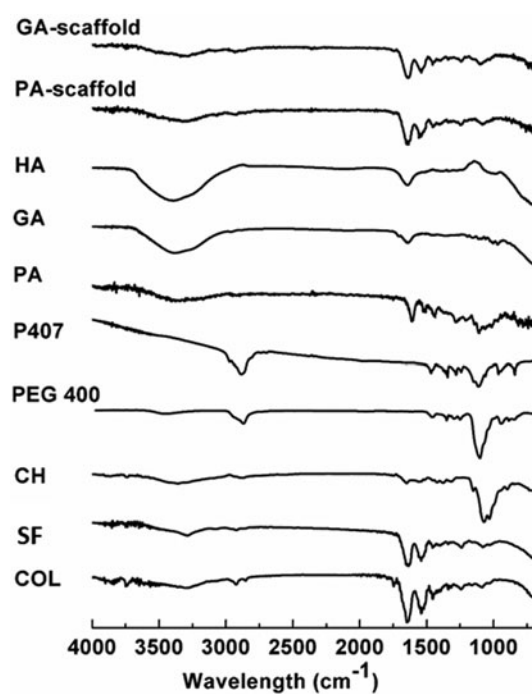


Figure 6. Fourier transform infrared spectroscopy spectra of raw materials, PA-scaffold, and GA-scaffold.

amide II band of scaffold, indicating that the amide groups may be involved in the crosslinking reaction to form Schiff bases.

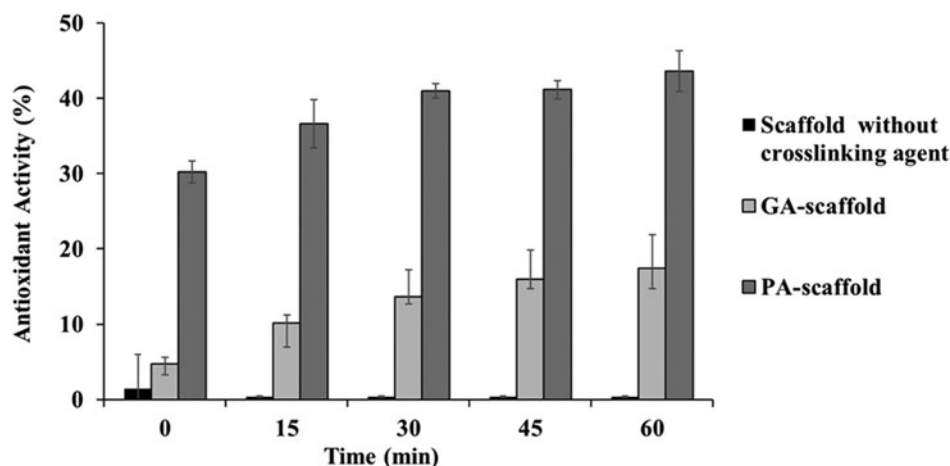


Figure 7. Antioxidant activity of the scaffolds as a function of time. *Statistical equals were found between PA-scaffold and GA-scaffold ($p > .05$) ($n = 3$; bar charts represent standard deviation values).

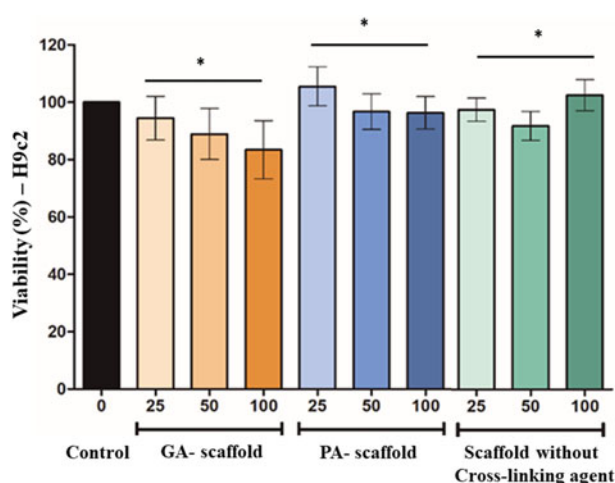


Figure 8. Results of MTT analyses, exposure to GA-scaffold, PA-scaffold, and scaffold without the crosslinking agent in H9c2 cells for 24 hours.

In vitro antioxidant activity

Figure 7 shows the antioxidant activity of the scaffold without a crosslinking agent, PA-scaffold, and GA scaffold. The analysis of the scaffold without a crosslinking agent was made as a control to know if the blend of polymer had antioxidant property. In the end, PA-scaffold showed 44% antioxidant activity, this is 2.6 times more than GA-scaffold (17%), and 121 times more the scaffolds without the crosslinking agent (0.36%).

Cell viability

Figure 8 shows results of MTT analyses, exposure to GA-scaffold, PA-scaffold, and scaffold without a cross-linking agent in H9c2 cells for 24 hours. The results showed that after 24 hours the cellular viability of exposure to GA was the only one that presented a decrease, about 15% with respect to the control, however, it was not significant. Regarding the exposure to PA-scaffold and GA-scaffold, and scaffold without crosslinking agent, viabilities $>90\%$ were observed. It was not possible at these concentrations to determine the IC50 (Figure 8).

Cytometer image

The results showed that PA-scaffold and GA-scaffold presented significant differences during the growth in relation to the control, after 48 and 72 hours, presenting a decrease of the cellular multiplication (Figure 9A). The graph of Figure 9B shows the cell growth curve of the different scaffolds, but these seem to return to normal after a period of 72 hours, as shown in Figure 9B.

Discussion

When suitable autologous tissue is injured or lacking, mostly the use of nonbiodegradable synthetic material to maintain the 3D structure and to increase the time of biodegradation in scaffolds to restore, and repair the tissue is associated with several disadvantages, such as the significant risk of thromboembolism, fibrosis, and calcification.

In the other hand, the use of biodegradable material to assure structural and biomechanical features that mimetic of the cardiac ECM has the inconvenience of the fast disintegration, generally, lesser than 8 weeks. Techniques to modulate the biomechanical and features properties of 3D porous scaffold based on biocompatible polymers, natural or synthetic, crosslinking agent, or by compressing hydrogels. In this manuscript, we associated the biocompatible and biodegradable, natural and synthetic, polymers, crosslinking agent, and plastic compression to obtain the dense lamellar scaffolds in such a way that new mechanical and biomechanical properties arise.

The requirements of such a scaffold are: (i) highly porous and 3D structures to allow cell and nutrient infiltration, (ii) proper biomechanical properties, (iii) the ability to disintegrate to nontoxic products and (iv) biocompatibility, allowing cells to attach and proliferate. The scaffolds were obtained with glutaraldehyde and PA as a crosslinking agent.

The mucoadhesion reflects the ability of a material to adhere to a biological substrate, and it is a crucial biomechanical property of scaffolds for tissue regeneration. The results of mucoadhesion shown in Figure 1A suggest that

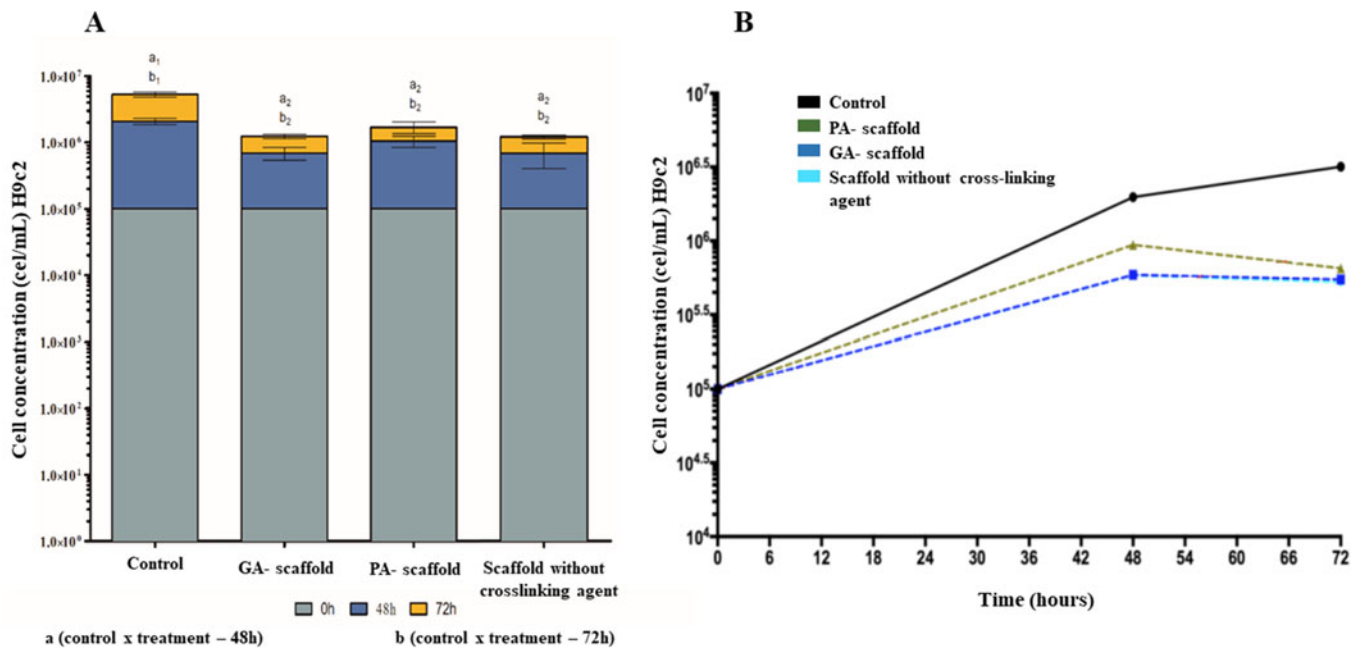


Figure 9. (A) Results on cell growth (H9c2) and (B) Cell growth curve (H9c2) after exposure to GA-scaffold, PA-scaffold, and scaffold without the crosslinking agent at 48 and 72 hours.

the mechanism of scaffold's mucoadhesion is due to HA, chitosan, and P407 properties into both formulations, that is, the presence of the PA and GA crosslinkers did not show the difference between the mucoadhesion studies ($p > .05$).

The interaction between mucus and mucin is a result of physical entanglement and secondary bonding, mainly H-bonding and van der Waals attraction, which according to the many authors, are mainly related to the following polymer properties: the capability to create strong H bonding, high molecular weight, sufficient chain flexibility, and surface load properties favoring spreading onto mucus.^[46]

Anionic polymers, carrying $-\text{COOH}$ groups, can form hydrogen bonds with the hydroxyl groups of the glycoprotein's oligosaccharide side chain. This group includes polymers such as HA. Cationic polymers carry a positively charged amine group and can, therefore, adhere to mucous due to ionic attraction to the sialic acid groups on the oligosaccharide side chain as chitosan. The interaction of non-ionic polymers is based on the interpenetration of the polymer chains followed by chain entanglement as P407.^[47] Thus, the mechanism of scaffold's mucoadhesion can be explained due to the HA, chitosan, and P407 into both formulations. In this case, the presence of PA and GA did not show the difference between the mucoadhesion studies ($p > .05$).

It is known that Young's modulus depends on the relative density and porosity of the scaffold, and of a constant related to the pore geometry. The linear elastic (Young's) modulus calculated from stress-strain analysis gives precisely the measure of the resistance of the struts to bending and buckling under compression.

Compressive properties are of greater interest when studying the impact of scaffold mechanics on cellular activity, because cells, through their action, tend to bend and buckle individual struts within the scaffold.^[48] The

analysis of results (Figure 1) shows that dense lamellar PA-scaffold could potentially be applied as heart patch materials in terms of stiffness.

The scaffolds to cardiac regeneration have been obtained by electrospinning using synthetic copolymers to improve Young's modulus.^[8,49,50] The results compilation found these authors showed that Young's modulus is a function of copolymer used. The choice of copolymers can modify the potential to obtain structurally and functionally competent cardiac tissue construct.^[46]

Engineered heart devices must develop systolic (contractive) force with suitable compliance, at the same time they must withstand diastolic (expansive) loads. The compliance is defined as $1/E$, where E is stiffness of the scaffold material should be that of the collagen matrix of the heart muscle. The fact of the scaffolds have not a contractile function is due to the stiffness of collagen fibers. The same property has been attributed at most biomaterials.^[8] As shown in Figure 1B, the plastic compression technique associated with a crosslinking was considered efficient to modulate the stiffness and proper physiomechanical properties of the scaffold produced with GA and PA.

The stress relaxation demonstrates the transient mechanical behavior of gels through the relative ability of the gel network to withstand the targeted strain. For stress relaxation tests, the fracture does not occur, and the energy intake during compression is not completely stored in the material. The value of maximum force (F_{max}) represents the initial firmness of the gel at 10% of compression strain. Hence, the gel strength and deformability depend on the number and the type of bonds within the gel network.^[51,52]

Figure 1C shows the stress relaxation curves for PA and GA scaffold. The slower relaxation for PA-scaffold characterized by deflection of the curve after reaching the maximum absorbed force ($F_{\text{max}} = 1.14\text{N}$), as a result of the

rigid network strand, however, flexible. The lower F_{\max} level (0.5 N) for GA-scaffold represents a stiffer and less flexible structure compared to PA-scaffold. This difference was attributed to store lower level of energy (GA-scaffold), due to the dissipated energy.

Figure 2A shows the rate of fluid uptake of scaffolds, whereas Figure 2B shows the fluid uptake by polymeric chain. Crosslinking is a primary factor decreasing the water absorption and retention of scaffolds, and the results of this study are in accordance with similar results.^[19,53,54] The water absorption of GA-scaffold was bigger than PA-scaffolds which suggests that PA treatment not only reduces the number of hydrophilic groups on the biopolymers of the formulation, which could bind water and to reduce the space between the chains.^[19,55] As a result, the capability of water absorption gradually decreases as the type of crosslinking agent. Collagen/chitosan scaffolds produced by freeze-drying and used carbodiimide and sodium tripolyphosphate as crosslinking agent.^[3] At the end of 14 days, the scaffolds showed weight loss in the range of 40–50%, in PBS medium. Thus, the PA as a natural polyphenolic component can crosslink proteins (collagen, rich in proline) through hydrogen bonding slowing down the biodesintegration of scaffolds.

Cardiac scaffolds must have as a particular quality a highly porous structure, with high rate open porous, anisotropic, and fully interconnected for providing a large surface area that will allow cell ingrowth, uniform cell distribution, and facilitate the neovascularization.^[56]

The morphological characteristics of PA-scaffold and GA-scaffold were obtained by μ CT and summarized in Table 2. The results analyzed shows that the PA-scaffold has the better morphological properties to cells proliferation (Figure 9).

Cell behavior is directly affected by the scaffold architecture (e.g., porosity, pore size, interconnectivity, anisotropy, and diameter of fibers), since the ECM provides cues that influence the specific integrin–ligand interactions between cells and the surrounding. The role of porosity and interconnectivity in scaffolds is to favor cell migration inside the porous structure, such that cell growth is facilitated while overcrowding is avoided. Besides, the pore size of scaffolds can influence the amount of glycosaminoglycan secretion and the expression of collagen gene markers.^[57]

The anisotropy is a product of plastic compression technique and is associated with lamellar characteristic on scaffolds. In a 3D perspective of the scaffold, the topographic anisotropy of the constructs is an essential factor in cells motility, alignment, and physiological functions due to cell capacity of cognizing the orientation and texture based on physical properties of scaffolds.^[56] The scaffold produced by our group using the PA as crosslinking agent showed appropriate morphology and size porous, this can favor the cellular adhesion and proliferation (Table 2 and Figure 9).

The permeability coefficients (PA-scaffold $7 \times 10^{-9} \text{ m}^2$ and GA-scaffold was $2 \times 10^{-10} \text{ m}^2$) are coherent with degree of anisotropy. The permeability can be characterized as a combination of essential parameters: (i) porosity, (ii) porous

size and distribution, (iii) porous interconnectivity, and (iv) porous orientation (anisotropy). In the last instance, the permeability of a scaffold is a property defining fluid flow through a porous material. Thus, as previously noted, the permeability of biological tissues and tissue-engineered scaffolds plays a significant role in nutrient and waste transport.^[36,58]

Differential scanning calorimetry (Figure 5) was used to measure the denaturation temperature (T_d) which correspond at a measure of crosslinking density. The DSC results gave a better understanding of the unfolding of protein under the influence of temperature (90 °C). The DSC plots depict an endothermic peak (220 °C) associated with a helix to coil transition, which indicates the extent of intermolecular crosslinking.^[42] In general, the miscibility of the polymers blend depends on the self-association and interassociation of hydrogen-bonding donor polymers.

The spectra of PA-scaffold and GA-scaffold (Figure 6) showed the crosslinking formation between COL-PA and COL-GA. The hydrogen bonding is the main mechanism of interaction between hydroxyl groups present in PA and amino and amide groups of COL. However, hydrophobic interactions were also proposed to explain the binding of polyphenols to proteins, which might occur through the association of their aromatic rings with proline residues.^[44]

Crosslinking of COL with GA involves the reaction of the free amine groups of lysine or hydroxylysine amino acid residues of the polypeptide chains with the GA aldehyde groups. More specifically, the first step of the reaction involves the nucleophilic addition of the ε -NH₂ groups to the carbonyl groups (C=O) of the aldehyde to form an unstable tetrahedral intermediate called carbinolamine. In a second step, protonation of the –OH group followed by loss of a water molecule yields the conjugated Schiff bases.^[29]

The antioxidant activity of PA-scaffold was 2.60 times more than GA scaffold (Figure 7). The evaluation of the antioxidant activity of scaffold needs to be considered when the polymers and crosslinking agent are projected for biomedical applications. Proanthocyanidins are known to possess antibacterial, antiviral, anti-inflammatory, antiallergic, and vasodilator actions.

Proanthocyanidins also has been shown to modulate the activity of regulatory enzymes including cyclooxygenase, lipooxygenase, protein kinase C, angiotensin-converting enzyme, hyaluronidase enzyme, and cytochrome P450 activities. Effectively, PA suppresses oxidative stress through repairing DNA damage, preventing lipid peroxidation, platelet aggregation, capillary's permeability and fragility; moreover, modulating signaling pathways (e.g., Nrf2, MAPKs, NF- κ B pathways) and, further, treat oxidative stress-related diseases like cardiovascular diseases, neurodegenerative disorders, metabolic diseases, skin disorders, and cancer.^[22,23]

There is an increasing interest toward studying natural and synthetic antioxidants to prevent the uncontrolled oxidation of lipids, proteins, and DNA caused by the development of various diseases like cardiac and cerebral ischemia, infection, and cardiovascular diseases.^[59] Our results confirm the ability of the PA to inhibit free radical moieties.

Utilization of PA in the scaffolds may have a striking effect on healing of tissues suffering from high oxidative stress especially due to infarction.

The in vitro study carried out here (Figure 9A and 9B) aimed to evaluate in a preliminary way the possible toxicity or lack of control of the cell cycle. Proanthocyanidins-scaffolds showed moderate wettability, and this improves the attachment, growth, and migration of cells since their surface has preferential absorption of cell-adhesive proteins. Finally, the surface roughness of PA-scaffold has an important influence on protein absorption and hence cell adhesion and migration upon implantation in vivo. Moreover, the microstructures of the PA-scaffolds obtained by our group showed good features to ensure the proliferation and migration cell for large extent time.

Chronic cytotoxicity is always of primary concern when designing biomedical devices using crosslinked collagen matrices. Proanthocyanidin is widely used as a food supplement, and its lack of toxicity has been extensively demonstrated. In addition, PA has been reported to pose antibacterial, antiviral, anticarcinogenic, anti-inflammatory, and antiallergic activities.^[21] The results of cytotoxicity and cell viability (Figures 8 and 9) showed that the material leads to an initial imbalance in the cells tested, but these seem to return to normal after a period of 72 hours. In Figure 9A and 9B, there is the apparent difference between exposed material and the control (without exposure), but no significant difference ($p < .05$) between the types (PA-scaffold, GA-scaffold, and scaffold without crosslinking agent). As no significant cell death was observed on exposure, it is concluded that the material does not lead to cell death but lead to an initial decrease in multiplication that is restored after 72 hours.

The PA-crosslinked scaffold could promote the cells attachment at the early stage after seeding. It can increase cell proliferation rate compared to the GA and uncross-linked scaffolds. In addition, it has been reported that PA-related polyphenols could stimulate the proliferation of normal cells and increase the synthesis of ECM, and PA-crosslinked collagenous materials could enhance the cell's ability to deposit collagen where collagen is widely known to play important role in cell adhesion and ECM formation.^[19]

Cytotoxicity assay using fibroblast cultures revealed that PA is ~ 120 times less toxic than GA, a currently used tissue stabilizer. In vitro degradation, a criterion often used to examine the degree of collagen crosslinking showed that fixed tissue was resistant to digestion by bacterial collagenase.^[21]

Conclusion

The choice of biomaterial and experimental condition for the design of these scaffolds was important parameter to assuring the biomimetic performance. The scaffolds obtained by plastic compression associated with crosslinking agent showed to be able to modulate the stiffness and suitable biomechanical properties to support the reverse modulation of the myocardium. The effect of crosslinking agent modified the biomechanical properties such as drilling,

flexibility, traction, and stress relaxation, but it did not modify the mucoadhesion property. The results of uptake saturation and weight loss suggest that PA-scaffold has a potential for mechanically support the native tissue during the necessary time for tissue regeneration. The antioxidant activity of PA-scaffold will have a more significant effect healthful to remodel native tissue that underwent oxidative stress. Both crosslinking agents did not influence in the H9c2 viability ($>90\%$), the H9c2 multiplication presenting a discreet decrease after 48 and 72 hours. However, as no significant cell death was observed on exposure, it is concluded that the scaffold did not lead to cell death but a small decrease in multiplication that was restored after 72 hours. Considering the anisotropic structure, the biomechanical properties, cellular compatibility, and protective action against reactive oxygen species, this study may provide a way to improve the inverse remodulation of heart tissue, after infarct acute of the myocardium.

Author contributions

T. F. R.A developed the study, organization, and discussion of results, and wrote the manuscript. J. F.S. and K.M.M.C. assisted in textural analyzation and swelling test. D.G. performed and analyzed the antioxidant activity. R.L. and T.G.C. performed and analyzed viability and multiplication cell. N.A., V.A.A, and F.B. provided the silk cocoons of *Bombyx mori*, and assisted in the extraction of silk fibroin. L. M.S. F. assisted with the cardiac discussion about biomimetic scaffolds. J. M.O.J. performed and analyzed the morphometric characteristic by computerized microtomography. P.S. and A.C.R performed the physical-chemical analyses. M.V.C. is head of LaBNUS and was responsible for project administration and general supervision of works. All authors reviewed and commented on the manuscript.

Conflicts of interest

The authors have no competing interests to declare.

Funding

Postgraduate Support Program for Private Education Institution – Coordination for the Improvement of Higher Education Personnel (Prosup-Capes) with financial support for scholarship. CNPq-Brazil: 425271/2016-1. FAPESP-Brazil 13432-0/2018. This work was supported by Conselho Nacional de Desenvolvimento Científico e Tecnológico; Coordenação de Aperfeiçoamento de Pessoal de Nível Superior; Fundação de Amparo à Pesquisa do Estado de São Paulo.

ORCID

Thais Alves  <http://orcid.org/0000-0002-3586-9457>
 Venancio Alves Amaral  <http://orcid.org/0000-0002-4617-2014>
 Denise Grotto  <http://orcid.org/0000-0002-8782-0436>
 Patricia Severino  <http://orcid.org/0000-0001-6527-6612>

References

- [1] Li, Y.; Zhang, D. Artificial Cardiac Muscle with or without the Use of Scaffolds. *Biomed Res. Int.* **2017**, Article ID 8473465, 15. DOI: [10.1155/2017/8473465](https://doi.org/10.1155/2017/8473465).
- [2] Eschenhagen, T.; Eder, A.; Vollert, I.; Hansen, A. Physiological Aspects of Cardiac Tissue Engineering. *AJP Heart Circ. Physiol.* **2012**, 303, H133–H143. DOI: [10.1152/ajpheart.00007.2012](https://doi.org/10.1152/ajpheart.00007.2012).
- [3] Martínez, A.; Blanco, M. D.; Davidenko, N.; Cameron, R. E. Tailoring Chitosan/Collagen Scaffolds for Tissue Engineering: Effect of Composition and Different Crosslinking Agents on Scaffold Properties. *Carbohydr. Polym.* **2015**, 132, 606–619. DOI: [10.1016/j.carbpol.2015.06.084](https://doi.org/10.1016/j.carbpol.2015.06.084).
- [4] Mao, A. S.; Mooney, D. J. Regenerative Medicine: Current Therapies and Future Directions. *Proc. Natl. Acad. Sci. U S A* **2015**, 112, 14452–14459. DOI: [10.1073/pnas.1508520112](https://doi.org/10.1073/pnas.1508520112).
- [5] O'Brien, F. J. Biomaterials & Scaffolds for Tissue Engineering. *Mater. Today* **2011**, 14, 88–95. DOI: [10.1016/S1369-7021\(11\)70058-X](https://doi.org/10.1016/S1369-7021(11)70058-X).
- [6] Naveed, M.; Han, L.; Khan, G. J.; Yasmeen, S.; Mikrani, R.; Abbas, M.; Cunyu, L.; Xiaohui, Z. Cardio-Supportive Devices (VRD & DCC Device) and Patches for Advanced Heart Failure: A Review, Summary of State of the Art and Future Directions. *Biomed. Pharmacother.* **2018**, 102, 41–54. DOI: [10.1016/j.biopha.2018.03.049](https://doi.org/10.1016/j.biopha.2018.03.049).
- [7] Karikkineth, B. C.; Zimmermann, W.-H. Myocardial Tissue Engineering and Heart Muscle Repair. *Curr. Pharm. Biotechnol.* **2013**, 14, 4–11. DOI: [10.2174/138920113804805322](https://doi.org/10.2174/138920113804805322).
- [8] Chen, Q. Z.; Bismarck, A.; Hansen, U.; Junaid, S.; Tran, M. Q.; Harding, S. E.; Ali, N. N.; Boccacini, A. R. Characterisation of a Soft Elastomer Poly(Glycerol Sebacate) Designed to Match the Mechanical Properties of Myocardial Tissue. *Biomaterials* **2008**, 29, 47–57. DOI: [10.1016/j.biomaterials.2007.09.010](https://doi.org/10.1016/j.biomaterials.2007.09.010).
- [9] Arpornmaeklong, P.; Pripatnanont, P.; Suwatwirote, N. Properties of Chitosan-Collagen Sponges and Osteogenic Differentiation of Rat-Bone-Marrow Stromal Cells. *Int. J. Oral Maxillofac. Surg.* **2008**, 37, 357–366. DOI: [10.1016/j.ijom.2007.11.014](https://doi.org/10.1016/j.ijom.2007.11.014).
- [10] Deng, C.; Zhang, P.; Vulesevic, B.; Kuraitis, D.; Li, F.; Yang, A. F.; Griffith, M.; Ruel, M.; Suuronen, E. J. A Collagen–Chitosan Hydrogel for Endothelial Differentiation and Angiogenesis. *Tissue Eng.* **2010**, 16, 3099–3109. DOI: [10.1089/ten.tea.2009.0504](https://doi.org/10.1089/ten.tea.2009.0504).
- [11] Lu, W.-N.; Lu, S.-H.; Wang, H.-B.; Li, D.-X.; Duan, C.-M.; Liu, Z.-Q.; Hao, T.; He, W.-J.; Xu, B.; Fu, Q. Functional Improvement of Infarcted Heart by Co-Injection of Embryonic Stem Cells with Temperature-Responsive Chitosan Hydrogel. *Tissue Eng.* **2009**, 15, 1437–1447. DOI: [10.1089/ten.tea.2008.0143](https://doi.org/10.1089/ten.tea.2008.0143).
- [12] Gobin, A. S.; Froude, V. E.; Mathur, A. B. Structural and Mechanical Characteristics of Silk Fibroin and Chitosan Blend Scaffolds for Tissue Regeneration. *J. Biomed. Mater. Res.* **2005**, 74, 465–473. DOI: [10.1002/jbm.a.30382](https://doi.org/10.1002/jbm.a.30382).
- [13] Bonafè, F.; Govoni, M.; Giordano, E.; Calderara, C. M.; Guarnieri, C.; Muscari, C. Hyaluronan and Cardiac Regeneration. *J. Biomed. Sci.* **2014**, 21, 100–113. DOI: [10.1186/s12929-014-0100-4](https://doi.org/10.1186/s12929-014-0100-4).
- [14] Hu, K.; Shi, H.; Zhu, J.; Deng, D.; Zhou, G.; Zhang, W.; Cao, Y.; Liu, W. Compressed Collagen Gel as the Scaffold for Skin Engineering. *Biomed. Microdevices* **2010**, 12, 627–635. DOI: [10.1007/s10544-010-9415-4](https://doi.org/10.1007/s10544-010-9415-4).
- [15] Brown, R. A.; Wiseman, M.; Chuo, C. B.; Cheema, U.; Nazhat, S. N. Ultrarapid Engineering of Biomimetic Materials and Tissues: Fabrication of Nano- and Microstructures by Plastic Compression. *Adv. Funct. Mater.* **2005**, 15, 1762–1770. DOI: [10.1002/adfm.200500042](https://doi.org/10.1002/adfm.200500042).
- [16] Mi, S.; Chen, B.; Wright, B.; Cannon, C. J. Plastic Compression of a Collagen Gel Forms a Much Improved Scaffold for Ocular Surface Tissue Engineering over Conventional Collagen Gels. *J. Biomed. Mater. Res.* **2010**, 95 A, 447–453. DOI: [10.1002/jbm.a.32861](https://doi.org/10.1002/jbm.a.32861).
- [17] Rich, H.; Odlyha, M.; Cheema, U.; Mudera, V.; Bozec, L. Effects of Photochemical Riboflavin-Mediated Crosslinks on the Physical Properties of Collagen Constructs and Fibrils. *J. Mater. Sci. Mater. Med.* **2014**, 25, 11–21. DOI: [10.1007/s10856-013-5038-7](https://doi.org/10.1007/s10856-013-5038-7).
- [18] Oryan, A.; Kamali, A.; Moshiri, A.; Baharvand, H.; Daemi, H. Chemical Crosslinking of Biopolymeric Scaffolds: Current Knowledge and Future Directions of Crosslinked Engineered Bone Scaffolds. *Int. J. Biol. Macromol.* **2018**, 107, 678–688. DOI: [10.1016/j.ijbiomac.2017.08.184](https://doi.org/10.1016/j.ijbiomac.2017.08.184).
- [19] Yang, Y.; Ritchie, A. C.; Everitt, N. M. Comparison of Glutaraldehyde and Proanthocyanidin Cross-Linked Scaffolds for Soft Tissue Engineering. *Mater. Sci. Eng. C* **2017**, 80, 263–273. DOI: [10.1016/j.msec.2017.05.141](https://doi.org/10.1016/j.msec.2017.05.141).
- [20] Shavandi, A.; Bekhit, A. E.-D. A.; Saeedi, P.; Izadifar, Z.; Bekhit, A. A.; Khademhosseini, A. Polyphenol Uses in Biomaterials Engineering. *Biomaterials* **2018**, 167, 91–106. DOI: [10.1016/j.biomaterials.2018.03.018](https://doi.org/10.1016/j.biomaterials.2018.03.018).
- [21] Han, B.; Jauregui, J.; Tang, B. W.; Nimni, M. E. Proanthocyanidin: A Natural Crosslinking Reagent for Stabilizing Collagen Matrices. *J. Biomed. Mater. Res.* **2003**, 65, 118–124. DOI: [10.1002/jbm.a.10460](https://doi.org/10.1002/jbm.a.10460).
- [22] Bagchi, D.; Sen, C. K.; Ray, S. D.; Das, D. K.; Bagchi, M.; Preuss, H. G.; Vinson, J. A. Molecular Mechanisms of Cardioprotection by a Novel Grape Seed Proanthocyanidin Extract. *Mutat. Res. Fundam. Mol. Mech. Mutagen* **2003**, 523–524, 87–97. DOI: [10.1016/S0027-5107\(02\)00324-X](https://doi.org/10.1016/S0027-5107(02)00324-X).
- [23] Bagchi, D.; Bagchi, M.; Stohs, S. J. Cellular Protection with Proanthocyanidins. *Ann. New York Acad. Sci.* **2002**, 270, 260–270. DOI: [10.1111/j.1749-6632.2002.tb02922.x](https://doi.org/10.1111/j.1749-6632.2002.tb02922.x).
- [24] Lee, J.; Sabatini, C. Glutaraldehyde Collagen Cross-Linking Stabilizes Resin–Dentin Interfaces and Reduces Bond Degradation. *Eur. J. Oral Sci.* **2017**, 125, 63–71. DOI: [10.1111/eos.12317](https://doi.org/10.1111/eos.12317).
- [25] Yap, L. S.; Yang, M. C. Evaluation of Hydrogel Composing of Pluronic F127 and Carboxymethyl Hexanoyl Chitosan as Injectable Scaffold for Tissue Engineering Applications. *Coll. Surf. B* **2016**, 146, 204–211. DOI: [10.1016/j.colsurfb.2016.05.094](https://doi.org/10.1016/j.colsurfb.2016.05.094).
- [26] Liu, Y.; Ma, L.; Gao, C. Facile Fabrication of the Glutaraldehyde Cross-Linked Collagen/Chitosan Porous Scaffold for Skin Tissue Engineering. *Mater. Sci. Eng. C* **2012**, 32, 2361–2366. DOI: [10.1016/j.msec.2012.07.008](https://doi.org/10.1016/j.msec.2012.07.008).
- [27] Likitamporn, S.; Magaraphan, R. Mechanical and Thermal Properties of Sericin/Pva/Bentonite Scaffold: Comparison between Uncrosslinked and Crosslinked. *Macromol. Symp.* **2014**, 337, 102–108. DOI: [10.1002/masy.201450312](https://doi.org/10.1002/masy.201450312).
- [28] Ho, H. O.; Lin, C. W.; Sheu, M. T. Diffusion Characteristics of Collagen Film. *J. Control. Release* **2001**, 77, 97–105. DOI: [10.1016/S0168-3659\(01\)00467-9](https://doi.org/10.1016/S0168-3659(01)00467-9).
- [29] Olde Damink, L. H. H.; Dijkstra, P. J.; Van Luyn, M. J. A.; Van Wachem, P. B.; Nieuwenhuis, P.; Feijen, J. Glutaraldehyde as a Crosslinking Agent for Collagen-Based Biomaterials. *J. Mater. Sci. Mater. Med.* **1995**, 6, 460–472. DOI: [10.1007/BF00123371](https://doi.org/10.1007/BF00123371).
- [30] Wei, Y.; Chang, Y.-H.; Liu, C.-J.; Chung, R.-J. Integrated Oxidized-Hyaluronic Acid/Collagen Hydrogel with β -TCP Using Proanthocyanidins as a Crosslinker for Drug Delivery. *Pharmaceutics* **2018**, 10, 37. DOI: [10.3390/pharmaceutics10020037](https://doi.org/10.3390/pharmaceutics10020037).
- [31] Choi, Y.; Kim, H.-J.; Min, K.-S. Effects of Proanthocyanidin, A Crosslinking Agent, on Physical and Biological Properties of Collagen Hydrogel Scaffold. *Restor. Dent. Endod.* **2016**, 41, 296–303. DOI: [10.5395/rde.2016.41.4.296](https://doi.org/10.5395/rde.2016.41.4.296).
- [32] Komatsu, D.; Aranha, N.; Chaud, M. V.; Júnior, J. M.; de, O.; Mistura, D. V.; Motta, A.; Duek, E. A. R. Characterization of Membrane of Poly (L,Co-D,L-Lactic Acid-Co-Trimethylene Carbonate) (PLDLA-Co-TMC) (50/50) Loaded with Silk Fibroin. *SDRP J. Biomed. Eng.* **2017**, 2, 1–11. DOI: [10.25177/JBE.2.1.1](https://doi.org/10.25177/JBE.2.1.1).

- [33] Alves, T. F. R.; Souza, J. F.; de, Severino, P.; Andréo Filho, N.; de Lima, R.; Filho, L. M. S.; Rai, M.; Oliveira, Jr., J. M.; Chaud, M. V. Dense Lamellar Scaffold as Biomimetic Materials for Reverse Engineering of Myocardial Tissue: Preparation, Characterization and Physiomechanical Properties. *J. Mater. Sci. Eng.* **2018**, 7, 494. DOI: [10.4172/2169-0022.1000494](https://doi.org/10.4172/2169-0022.1000494).
- [34] Rebelo, M. A.; Chaud, M. V.; Balcão, V. M.; Vila, M. M. D. C.; Aranha, N.; Yoshida, V. M. H.; Alves, T. F.; Oliveira, Jr., J. M. Chitosan-Based Scaffolds for Tissue Regeneration: Preparation and Microstructure Characterization. *Eur. J. Biomed. Pharm. Sci.* **2016**, 3, 15–24.
- [35] Gilmore, J.; Yin, F.; Burg, K. J. L. Evaluation of Permeability and Fluid Wicking in Woven Fiber Bone Scaffolds. *J. Biomed. Mater. Res.* **2019**, 107, 306–313. DOI: [10.1002/jbm.b.34122](https://doi.org/10.1002/jbm.b.34122).
- [36] Varley, M. C.; Neelakantan, S.; Clyne, T. W.; Dean, J.; Brooks, R. A.; Markaki, A. E. Cell Structure, Stiffness and Permeability of Freeze-Dried Collagen Scaffolds in Dry and Hydrated States. *Acta Mater.* **2016**, 33, 166–174. DOI: [10.1016/j.actbio.2016.01.041](https://doi.org/10.1016/j.actbio.2016.01.041).
- [37] Alves, T.; Souza, J.; Rebelo, M.; Pontes, K.; Santos, C.; Lima, R.; Jozala, A.; Grotto, D.; Severino, P.; Rai, M.; Chaud, M. Formulation and Evaluation of Thermoresponsive Polymeric Blend as a Vaginal Controlled Delivery System. *J. Sol-Gel Sci. Technol.* **2018**, 86, 536–552. DOI: [10.1007/s10971-018-4662-6](https://doi.org/10.1007/s10971-018-4662-6).
- [38] Alves, T. F. R.; Chaud, M. V.; Grotto, D.; Jozala, A. F.; Pandit, R.; Rai, M.; dos Santos, C. A. Association of Silver Nanoparticles and Curcumin Solid Dispersion: Antimicrobial and Antioxidant Properties. *AAPS PharmSciTech.* **2018**, 19, 225. DOI: [10.1208/s12249-017-0832-z](https://doi.org/10.1208/s12249-017-0832-z).
- [39] Rheder, D. T.; Guilger, M.; Bilesky-José, N.; Germano-Costa, T.; Pasquoto-Stigliani, T.; Gallep, T. B. B.; Grillo, R.; Carvalho, C. d S.; Fraceto, L. F.; Lima, R. Synthesis of Biogenic Silver Nanoparticles Using *Althaea officinalis* as Reducing Agent: Evaluation of Toxicity and Ecotoxicity. *Sci. Rep.* **2018**, 8, 1–11. DOI: [10.1038/s41598-018-30317-9](https://doi.org/10.1038/s41598-018-30317-9).
- [40] de Mulder, E. L. W.; Buma, P.; Hannink, G. Anisotropic Porous Biodegradable Scaffolds for Musculoskeletal Tissue Engineering. *Materials (Basel)* **2009**, 2, 1674–1696. DOI: [10.3390/ma2041674](https://doi.org/10.3390/ma2041674).
- [41] Silva, A. M. H. d.; Alves, J. M.; Silva, O. L. d.; Silva Junior, N. F. d. Two and Three-Dimensional Morphometric Analysis of Trabecular Bone Using X-Ray Microtomography (ΜCT). *Rev. Bras. Eng. Bioméd.* **2014**, 30, 93–101. DOI: [10.1590/rbeb.2014.011](https://doi.org/10.1590/rbeb.2014.011).
- [42] Lakra, R.; Kiran, M. S.; Usha, R.; Mohan, R.; Sundaresan, R.; Korrapati, P. S. Enhanced Stabilization of Collagen by Furfural. *Int. J. Biol. Macromol.* **2014**, 65, 252–257. DOI: [10.1016/j.ijbio-mac.2014.01.040](https://doi.org/10.1016/j.ijbio-mac.2014.01.040).
- [43] Hendradi, E.; Hariyadi, D. M.; Adrianto, M. F. The Effect of Two Different Crosslinkers on In Vitro Characteristics of Ciprofloxacin-Loaded Chitosan Implants. *Res. Pharm. Sci.* **2018**, 13, 38–46. DOI: [10.4103/1735-5362.220966](https://doi.org/10.4103/1735-5362.220966).
- [44] Vidal, C. M. P.; Zhu, W.; Manohar, S.; Aydin, B.; Keiderling, T. A.; Messersmith, P. B.; Bedran-Russo, A. K. Collagen-Collagen Interactions Mediated by Plant-Derived Proanthocyanidins: A Spectroscopic and Atomic Force Microscopy Study. *Acta Biomater.* **2016**, 41, 110–118. DOI: [10.1016/j.actbio.2016.05.026](https://doi.org/10.1016/j.actbio.2016.05.026).
- [45] Nematollahi, Z.; Tafazzoli-Shadpour, M.; Zamanian, A.; Seyed-salehi, A.; Mohammad-Behgam, S.; Ghorbani, F.; Mirahmadi, F. Fabrication of Chitosan Silk-Based Tracheal Scaffold Using Freeze-Casting Method. *Iran. Biomed. J.* **2017**, 21, 228–239. DOI: [10.18869/acadpub.ijb.21.4.228](https://doi.org/10.18869/acadpub.ijb.21.4.228).
- [46] Mackie, A. R.; Goycoolea, F. M.; Menchicchi, B.; Caramella, C. M.; Saporito, F.; Lee, S.; Stephansen, K.; Chronakis, I. S.; Hiorth, M.; Adamczak, M.; et al. Innovative Methods and Applications in Mucoadhesion Research. *Macromol. Biosci.* **2017**, 17, 1600534. DOI: [10.1002/mabi.201600534](https://doi.org/10.1002/mabi.201600534).
- [47] Davidovik-Pinhas, M.; Bianco-Peled, H. Drug Delivery Systems Based on Mucoadhesive Polymers. In *Active Implants and Scaffolds for Tissue Regeneration*; Zilberman, M., Ed.; Springer-Verlag: Berlin, Heidelberg, **2010**; pp 439–456. DOI: [10.1007/8415_2010_39](https://doi.org/10.1007/8415_2010_39).
- [48] Davidenko, N.; Schuster, C. F.; Bax, D. V.; Raynal, N.; Farndale, R. W.; Best, S. M.; Cameron, R. E. Control of Crosslinking for Tailoring Collagen-Based Scaffolds Stability and Mechanics. *Acta Biomater.* **2015**, 25, 131–142. DOI: [10.1016/j.actbio.2015.07.034](https://doi.org/10.1016/j.actbio.2015.07.034).
- [49] Ravichandran, R. Cardiogenic Differentiation of Mesenchymal Stem Cells on Elastomeric Poly (Glycerol Sebacate)/Collagen Core/Shell Fibers. *World J. Cardiol.* **2013**, 5, 28. DOI: [10.4330/wjc.v5.i3.28](https://doi.org/10.4330/wjc.v5.i3.28).
- [50] Kai, D.; Prabhakaran, M. P.; Jin, G.; Ramakrishna, S. Guided Orientation of Cardiomyocytes on Electrospun Aligned Nanofibers for Cardiac Tissue Engineering. *J. Biomed. Mater. Res.* **2011**, 98 B, 379–386. DOI: [10.1002/jbm.b.31862](https://doi.org/10.1002/jbm.b.31862).
- [51] Tan, T. C.; Foo, W. T.; Liong, M. T.; Easa, A. M. Comparative Assessment of Rheological Properties of Gelatin or Gellan in Maize Starch – Egg White Composite Gels. *J. King Saud Univ. Sci.* **2014**, 26, 311–322. DOI: [10.1016/j.jksus.2014.02.001](https://doi.org/10.1016/j.jksus.2014.02.001).
- [52] Ortolani, E.; Quadrini, F.; Bellisario, D.; Santo, L.; Polimeni, A.; Santarsiero, A. Mechanical Qualification of Collagen Membranes Used in Dentistry. *Ann. Ist. Super. Sanita* **2015**, 51, 229–235. DOI: [10.4415/ANN_15_03_11](https://doi.org/10.4415/ANN_15_03_11).
- [53] Gupta, K. C.; Jabrail, F. H. Glutaraldehyde and Glyoxal Cross-Linked Chitosan Microspheres for Controlled Delivery of Centchroman. *Carbohydr. Res.* **2006**, 341, 744–756. DOI: [10.1016/j.carres.2006.02.003](https://doi.org/10.1016/j.carres.2006.02.003).
- [54] Bigi, A.; Cojazzi, G.; Panzavolta, S.; Rubini, K.; Roveri, N. Mechanical and Thermal Properties of Gelatin Films at Different Degrees of Glutaraldehyde Crosslinking. *Biomaterials* **2001**, 22, 763–768. DOI: [10.1016/S0142-9612\(00\)00236-2](https://doi.org/10.1016/S0142-9612(00)00236-2).
- [55] Trifković, K.; Milašinović, N.; Djordjević, V.; Zdunić, G.; Kalagasidis Krušić, M.; Knežević-Jugović, Z.; Šavikin, K.; Nedović, V.; Bugarski, B. Chitosan Crosslinked Microparticles with Encapsulated Polyphenols: Water Sorption and Release Properties. *J. Biomater. Appl.* **2015**, 30, 618–631. DOI: [10.1177/0885328215598940](https://doi.org/10.1177/0885328215598940).
- [56] Dhandayuthapani, B.; Yoshida, Y.; Maekawa, T.; Kumar, D. S. Polymeric Scaffolds in Tissue Engineering Application: A Review. *Int. J. Polym. Sci.* **2011**, 2011, 19, 290602. DOI: [10.1155/2011/290602](https://doi.org/10.1155/2011/290602).
- [57] Loh, Q. L.; Choong, C. Three-Dimensional Scaffolds for Tissue Engineering Applications: Role of Porosity and Pore Size. *Tissue Eng. Part B Rev.* **2013**, 19, 485–502. DOI: [10.1089/ten.teb.2012.0437](https://doi.org/10.1089/ten.teb.2012.0437).
- [58] O'Brien, F. J.; Harley, B. A. A.; Waller, M. A. A.; Yannas, I. V. V.; Gibson, L. J. The Effect of Pore Size on Permeability and Cell Attachment in Collagen Scaffolds for Tissue Engineering. *R. Coll. Surg. Irel.* **2007**, 15, 3–17.
- [59] Baheiraei, N.; Yeganeh, H.; Ai, J.; Gharibi, R.; Azami, M.; Faghihi, F. Synthesis, Characterization and Antioxidant Activity of a Novel Electroactive and Biodegradable Polyurethane for Cardiac Tissue Engineering Application. *Mater. Sci. Eng. C* **2014**, 44, 24–37. DOI: [10.1016/j.msec.2014.07.061](https://doi.org/10.1016/j.msec.2014.07.061).